Bulletin of the Seismological Society of America, Vol. 69, No. 4, pp. 1011–1026, August 1979

THE STABILIZATION OF SLIP ON A NARROW WEAKENING FAULT ZONE BY COUPLED DEFORMATION-PORE FLUID DIFFUSION

BY J. W. RUDNICKI

ABSTRACT

The transient stabilization of rapid slip on a very narrow weakening fault zone by the coupling of the deformation with pore fluid diffusion is investigated. More specifically, the fault zone is assumed to be so narrow that it can be idealized as a planar surface and the constitutive law is specified as a relation between stress on the fault τ_{flt} and relative slip δ. The study considers only the stabilizing effect due to the time dependent response of the fluid-infiltrated elastic material surrounding the fault: the response is elastically stiffer for load alterations which are too rapid to allow for fluid mass diffusion between neighboring material elements (undrained conditions) than for those which occur so slowly that the local pore fluid pressure is constant (drained conditions). Calculations are performed to determine the length of the precursory period (the period of self-driven accelerating slip prior to dynamic instability) by assuming that the near-peak τ_{flt} versus δ relation is parabolic and that the far-field tectonic stress rate is constant. An important result of the calculations is that the duration of the precursory period is predicted to decrease with increasing fault length for a plausible range of material parameters. Although this appears to disagree with results based on simple dimensional considerations, the result is due to the dependence of the constitutive law on a characteristic sliding distance necessary to reduce τ_{flt} from peak to residual value. Calculated precursor times are very short, typically less than a few days for fault lengths of 1 to 5 km, a tectonic stress rate of 0.1 bar/year, and field diffusivities of 0.1 to 1.0 m^2/sec. The results are, however, sensitive to details of the τ_{flt} versus δ relation which are, at present, poorly known.

INTRODUCTION

The diffusion of pore fluid has been suggested as a factor contributing to earthquake precursory phenomena. Although the initial interest in the role of pore-fluid diffusion primarily concerned its possible connection with purported observations of seismic-wave travel-time anomalies [e.g., Nur, 1972; Scholz *et al.*, 1973; Anderson and Whitcomb, 1975] Rice and Rudnicki (1979) (hereafter abbreviated as RR) have emphasized that the coupling of deformation with pore-fluid diffusion may be important in controlling the time scale of precursory deformation even when circumstances are not favorable for wave-speed alterations. More specifically, RR demonstrated that the coupling of deformation with pore-fluid diffusion can stabilize incipient rupture and give rise to a precursory period of quasi-static but accelerating deformation for plausible ranges of constitutive parameters.

There are two separate mechanisms for the transient stabilization of faulting by the mechanical action of pore fluids (Rice and Cleary, 1976). The first mechanism is that the presence of an infiltrating fluid in an otherwise linear elastic porous solid causes the response to applied loads to be time-dependent. Specifically, the response is *elastically* stiffer for load alterations which are rapid by comparison to the time scale of pore-fluid diffusion (undrained conditions) than for those which occur more slowly (drained conditions). During undrained conditions there is insufficient time

Present address: Department of Theoretical & Applied Mechanics, University of Illinois, Urbana, Illinois 61801.

for diffusive mass flux so that fluid-mass content of material elements is constant whereas for drained conditions the pore fluid diffuses in response to applied loads to keep the local pore-fluid pressure constant. The second mechanism of stabilization has been termed dilatant hardening and it arises from the tendency of brittle rock to dilate or increase the volume of pore space when sheared inelastically. If this dilation occurs more rapidly than fluid-mass diffusion into the newly created pore space, the local pore-fluid pressure decreases. Consequently, the effective compressive stress (total stress minus pore-fluid pressure) increases and inhibits further inelastic deformation due to extension of microcracks and frictional sliding on microcrack surfaces.

The study of these stabilizing mechanisms by RR was based on an inclusion model of faulting which was suggested by Rudnicki (1977). In this model, a zone of material (the inclusion) is considered to deform inelastically, and in particular to strain-soften, whereas the surrounding material remains nominally elastic. The rock mass is loaded by far-field stresses or strains, assumed to be of tectonic origin, and the inclusion material is driven past peak stress. Rudnicki (1977) identified the inception of seismic faulting with the point at which no further quasi-static deformation of this system is possible and a dynamic *runaway* of the inclusion strain occurs.

In order to incorporate the effects of pore fluids in this model, RR employed the solution of Rice *et al.* (1978) for the deformation of a spherical inclusion in a fluid-infiltrated porous elastic solid. Thus, the results are rigorous only for the case of a spherical inclusion. Although they estimated the results for more narrow zones by a suitable modification of parameters, they pointed out that these must be interpreted with caution. Fault zones observed in the field, however, are frequently very narrow (although these narrow zones may be the final result of instability in a process of inelastic deformation in a larger volume of material), and faulting is often idealized as slip on a planar surface. In this case, it is more appropriate to state the constitutive law as a relation between stress and relative sliding on the fault surface rather than between stress and strain.

The purpose of this paper is to study in a very simple way the stabilizing effects of the pore fluid for a very narrow zone and especially to assess differences between the time scale of precursory processes for inclusion zones and very narrow zones. Only the time-dependent stiffness effect will be analyzed. For convenience, the analysis will be restricted to the case of plane strain and will employ the solution of Rice and Cleary (1976) for a dislocation [also obtained by Booker (1974) for the special case of incompressible constituents] in a fluid-infiltrated porous elastic solid. Despite the simplicity of the analysis, one significant result is that the precursor time, as defined by RR, may decrease with increasing size of the zone for a representative range of material parameters. This result is in contrast to those based on simple dimensional considerations (Scholz *et al.*, 1973; Anderson and Whitcomb, 1975) and to those of RR. Although RR demonstrate that the precursor time does not generally scale with diffusion time L^2/c, where L is a characteristic length and c is diffusivity, the precursor time in their results does increase with increasing fault length. Nevertheless, the result obtained here is shown to be the proper limit of the inclusion model for very narrow zones.

The present analysis like that of RR considers a zone of inelasticity or slip which is fixed in size. For a very narrow zone, however, the strong-stress concentration at the edge of the zone may initiate spreading. Thus, models of spreading zones of slip are pertinent, particularly in situations of continuing slip on well established fault

zones. Rice and Simons (1976) have studied the stabilization of a spreading shear fault by time-dependent response of the surrounding material and Rice (1977) has discussed the coupled deformation-diffusion effects for a spreading zone of dilatancy on the basis of an earlier (Rice, 1973) one-dimensional model for shear-band propagation in overconsolidated clay slopes. Because of the mathematical complexity, results for spreading slip zones have been obtained only for very simple loadings. In contrast, the present analysis, although limited like that of RR to zones of inelasticity which are fixed in size, explores coupled deformation-diffusion effects for nonlinear relations between stress and slip or strain.

In the next section, the model will be discussed in more detail. The onset of runaway instability and the effects of the coupling of the pore-fluid diffusion with the deformation will be discussed qualitatively by means of a graphical analysis introduced by Rice (1977). Next, the relevant results of Rice and Cleary (1976) will be reviewed and then used to derive an integral equation for the time-dependent slip on the fault. This integral equation is solved numerically to determine the precursor time, the results are compared to those of RR, and possible implications for detecting earthquake precursors are discussed.

Model for Slip on a Narrow Fault

The discussion in the first part of this section follows that of Rice (1977). Consider a narrow fault zone which is idealized as a planar surface. The fault zone is embedded in nominally elastic material with shear modulus G and Poisson's ratio ν (Figure 1). The rock mass is loaded by far-field stresses which, for convenience, are taken to be the single shear stress τ_∞, whereas the stress sustained by the fault surface is τ_{flt}. If τ_{flt} is uniform and the fault surface is circular of radius L, then the relative displacement of the two sides is

$$\delta = \frac{4(1-\nu)}{\pi(2-\nu)}(2L)\frac{\tau_\infty - \tau_{flt}}{G}[1 - r^2/L^2]^{1/2}$$

where r is the distance from the center. If the fault surface is, instead, an infinite strip of width $2L$ (plane-strain geometry)

$$\delta = (1-\nu)(2L)\frac{\tau_\infty - \tau_{flt}}{G}[1 - r^2/L^2]^{1/2}.$$

Because the displacements are nonuniform, it is more convenient to work with the average displacements

$$\bar{\delta} = \xi(2L)(\tau_\infty - \tau_{flt})/G \tag{1}$$

where

$$\xi = 8(1-\nu)/3\pi(2-\nu) \tag{2}$$

for the circular geometry and

$$\xi = \pi(1-\nu)/4 \tag{3}$$

for plane strain. These formulas have been given by Rice (1977). If $\bar{\delta}$ is related to τ_{flt} by a constitutive law, equation (1) is for average slip on the fault as a function of

τ_∞. Thus, equation (1) is analogous to the "Eshelby relations" employed by Rudnicki (1977) and RR in their analyses of inclusion models for faulting.

Rice (1977) has suggested a simple graphical interpretation of equation (1) which is shown in Figure 2. The line represented by equation (1), which will be termed the Eshelby line, is drawn through the appropriate value of τ_∞ on the stress axis. The intersection of this line with the τ_{flt} versus $\bar{\delta}$ curve yields the values of stress and slip on the fault. As depicted in Figure 2a, τ_{flt} is always less than τ_∞ and consequently the fault is weaker than the surrounding material. However, Rice (1977) has pointed out that the graphical construction applies in the same way if the τ_{flt} versus $\bar{\delta}$ curve is drawn to the left of the τ axis (Figure 2b) where the slip on the fault is now measured relative to that for the unloaded state in the far-field. In this case, $\tau_{flt} > \tau_\infty$ and the fault has greater resistance to the imposed far-field deformation than

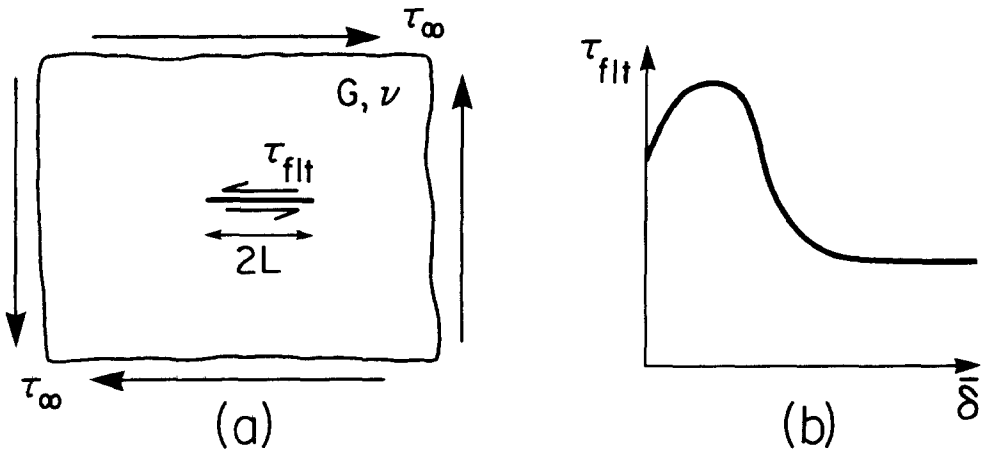

FIG. 1. (a) Model of a fault zone of length $2L$ embedded in nominally elastic material of shear modulus G and Poisson's ration ν. Loading is by far-field stresses τ_∞. (b) Relation between stress on the fault (τ_{flt}) and relative slip ($\bar{\delta}$) of the fault surface.

does the surrounding material. In either case, as τ_∞ increases, the stress on the fault traverses the τ_{flt} versus $\bar{\delta}$ curve (Figure 2c). After peak stress, there occurs a point (A in Figure 2c) at which the Eshelby line is tangent to the stress-displacement curve. At this point, no further quasi-static increase of τ_∞ is possible and there is a dynamic runaway of slip on the fault. The increases of τ_∞ are shown in equal increments in Figure 2c and the corresponding increments of $\bar{\delta}$ illustrate that the approach to instability is marked by an increased rate of fault slip. This is a general precursory effect and the accompanying increase in surface displacement rate has been studied in detail for long strike-slip earthquakes by Stuart (1979a) and by Stuart and Mavko (1979) and for the San Fernando thrust earthquake by Stuart (1979b). However, as in the case of the inclusion model (RR), the pre-instability acceleration of slip is more dramatic if pore-fluid effects are present.

It is evident from Figure 2 that the slope of the Eshelby line reflects the stiffness of the material surrounding the fault. However, the situation for a very narrow fault zone differs slightly from that for an inclusion zone because the stiffness of the surrounding material depends on the length of the zone. Specifically, the stiffness is inversely proportional to the length of the fault zone. (If the inclusion was considered to be embedded in a finite body and its length was comparable to the distance to

the boundaries, the effective stiffness of the surroundings would depend on the inclusion length, but presumably, this dependence would differ from that for the narrow zone of the same length.)

The onset of instability can be delayed by increasing the stiffness of the surrounding material, i.e., making the Eshelby line steeper. This is precisely the situation if the surrounding material is fluid-infiltrated: The increased rate of displacement as instability is approached causes the surrounding material to respond in stiffer, undrained fashion; in this case, the equation of the Eshelby line is given by equation (1) with the Poisson's ratio for undrained response ν_u substituted for ν. Because $\nu_u > \nu$ (Rice and Cleary, 1976), the Eshelby line is steeper. Although instability is delayed beyond point A (Figure 3a), if the slope of the τ_{flt} versus $\bar{\delta}$ curve continues to decrease, the curve eventually becomes tangent to the Eshelby line for undrained response, and instability ultimately occurs at point B. It is, of course, possible that the slope of the τ_{flt} versus $\bar{\delta}$ curve does not decrease monotonically from A to B but, instead, begins to increase at an intermediate point. In this case, a period of

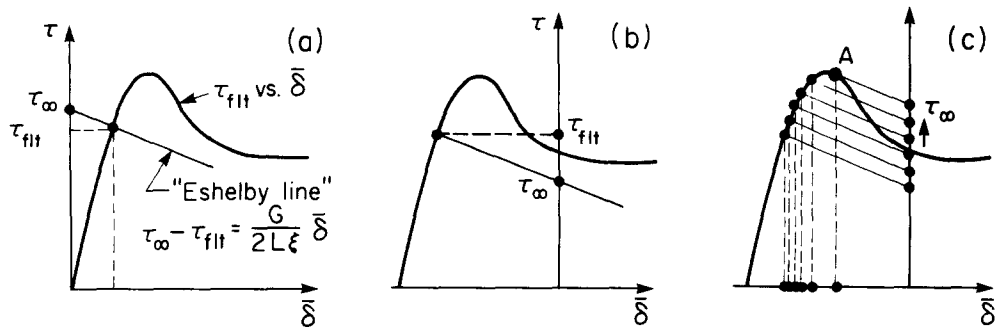

FIG. 2. (a) The "Eshelby line" relates the stress (τ_{flt}) and slip ($\bar{\delta}$) on the fault to the far-field stress τ_∞. (b) Seismic gap interpretation. (c) Approach to instability. Increase of τ_∞ in equal increments illustrates acceleration of slip $\bar{\delta}$ as instability (A) is approached (after Rice, 1977).

accelerated slip (in the sense described above) would not be followed by an instability. This example suggests the way in which processes of fault slip may be sensitive to details of the constitutive behavior.

If it is assumed that after instability the system simply comes to rest in the next equilibrium position based on the short-time or undrained response (C in Figure 3b), the construction in Figure 3b also predicts an amount of afterslip as the response relaxes from undrained conditions. This afterslip would correspond to the slip from C to D, at least if the relaxation rate is much greater than rate of increase of τ_∞. It is also worth remarking that the qualitative descriptions in Figures 2 and 3 are not limited to effects arising from pore-fluid diffusion, but may be applied to other situations of time-dependent behavior in which the limiting long-time and short-time responses are approximately elastic.

The dilatant hardening effect also has a simple interpretation in terms of the graphical construction in Figure 2. The decrease in pore-fluid pressure caused by the dilatancy which accompanies slip in the fault zone results in an increase of effective stress (total stress minus pore-fluid pressure) if the decrease in pore-fluid pressure occurs more rapidly than it can be alleviated by fluid diffusion. This increase in effective stress in response to rapid slip as point A (Figure 2) is approached will inhibit further inelastic deformation due to frictional sliding in the

fault zone. This process is reflected by a local increase in the slope of the τ_{flt} versus $\bar{\delta}$ curve near point A.

In the next section, the equations necessary to study more carefully the evolution of the system from A to B will be described for the case of stabilization by the time-dependent stiffness effect. In particular, it is of interest to calculate the length of time necessary to traverse the τ_{flt} versus $\bar{\delta}$ curve from A to B. Because the time scale of deformation during this period is set by pore-fluid diffusion and, consequently, is much more rapid than the tectonic deformation rate, it may be possible to observe precursory effects.

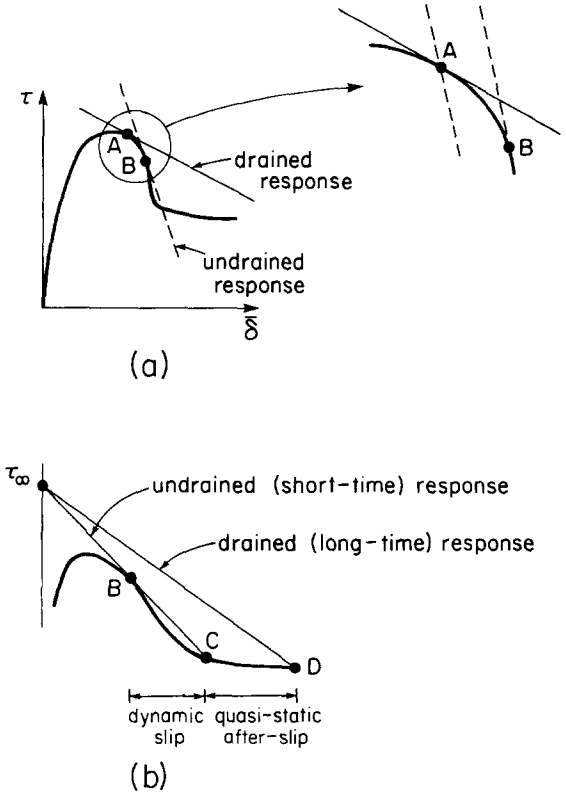

FIG. 3. (a) Stabilization of faulting from A to B by time-dependent stiffness of surroundings. Stiffness changes are exaggerated for illustration. (b) Quasistatic afterslip from C to D as the material surrounding the fault relaxes from undrained to drained response. Assumes τ_∞ = constant and that system takes on next equilibrium position (C) after instability (D).

ANALYSIS OF COUPLED DEFORMATION-DIFFUSION

The analysis will employ the solution for an edge dislocation suddenly introduced into an elastic porous fluid-infiltrated solid. This solution was derived for the special case of incompressible constituents by Booker (1974) and used to study the time-dependent redistribution of stress after faulting. Rice and Cleary (1976), in the course of establishing fundamental solutions for plane strain, obtained the edge dislocation solution for fully compressible constituents. Cleary (1977) has obtained the corresponding three-dimensional solution for a point dislocation.

The time-dependent shear stress $\tau(x, t)$ at a point x on the axis $y = 0$ due to an

edge dislocation having a Burgers vector of magnitude δ which is introduced on the x axis at x' and at time t' is (Rice and Cleary, 1976)

$$\tau(x, t) = \frac{G}{2\pi(1 - \nu_u)} \frac{\delta}{(x - x')} L[(x - x')^2/4c(t - t')], \qquad t > t' \tag{4}$$

where G is the shear modulus, ν_u is the Poisson's ratio for undrained response (constant fluid mass in material elements), c is the diffusivity,

$$L(z) = 1 - (\nu_u - \nu)z^{-1}(1 - e^{-z})/(1 - \nu),$$

and ν is Poisson's ratio for drained response (local pore-fluid pressure is constant). For very short times ($t \simeq t'$) the response is undrained, $L(\infty) = 1$, and equation (4) reduces to the usual elasticity result with ν_u as Poisson's ratio

$$\tau(x, t \simeq t') = \frac{G}{2\pi(1 - \nu_u)} \frac{\delta}{(x - x')}.$$

On the other hand, for very long times ($t \gg t'$), the response is drained, $L(0) = (1 - \nu_u)/(1 - \nu)$ and

$$\tau(x, t \gg t') = \frac{G}{2\pi(1 - \nu)} \frac{\delta}{(x - x')},$$

where the appropriate Poisson's ratio is now the drained value.

If the dislocations are continuously distributed in time and along a segment S of the x axis, the stress is

$$\tau(x, t) = \tau_\infty + \frac{G}{2\pi(1 - \nu_u)} \int_{-\infty}^{t} \int_S \frac{\partial^2 \delta(x', t')}{\partial x' \partial t'} \frac{1}{x - x'} L\left[\frac{(x - x')^2}{4c(t - t')}\right] dx'\, dt' \tag{5}$$

where τ_∞ is a uniform stress in the far-field and $(\partial^2\delta/\partial x'\partial t')\, dx'\, dt'$ is the net dislocation accumulated in time dt' and space dx'. If the stress on the fault surface is a function of the relative slip, i.e.

$$\tau(x, t) = \tau_{fit}[\delta(x, t)] \text{ on } S \tag{6}$$

then equation (5) is an integral equation for the slip on the fault surface. In general, the solutions to such equations are not unique unless a subsidiary condition is specified (Bilby and Eshelby, 1968; Muskhelishvili, 1953) e.g., that displacements outside the dislocation are single valued and that a Burgers' circuit around S encloses no net entrapped dislocation.

Unfortunately, when the constitutive relation, equation (6), is nonlinear, equations such as (5) are difficult to solve numerically (Cleary, 1976) even when the time-dependent effects due to pore-fluid diffusion are neglected. Therefore, matters are much simplified by considering two discrete dislocations at $x' = \pm a$. The dislocations are of equal magnitude but have opposite orientations, and they vary continuously in time. Also, the stress at the center of the dislocations is assumed to be represent-

ative of the stress sustained by the fault, i.e., $\tau(x = 0, t) = \tau_{flt}$. With these simplifications and the substitution of equation (6), equation (5) becomes

$$\tau_{flt}[\delta(\theta)] = \tau_\infty(\theta) - \frac{G}{(1 - \nu_u)\pi a} \int_{-\infty}^{\theta} \frac{d\delta}{d\theta'}(\theta') L(\theta - \theta')\, d\theta' \tag{7}$$

where $\theta = 4ct/a^2$ is time nondimensionalized by the diffusion time $a^2/4c$. The separation between the dislocations 2a is chosen so that for drained response, equation (7) reduces to the expression for the relative displacement at the center of a crack-like fault of length $2L$ which sustains a uniform stress τ_{flt}

$$\delta = (2L)(1 - \nu)(\tau_\infty - \tau_{flt})/G. \tag{8}$$

Thus, $a = 2L/\pi$ in order to simulate more closely a crack-like fault. Although these simplifications seem drastic, the constitutive parameters are so poorly known that it does not seem sensible to consider overly detailed models. Moreover, equation (8) differs from equation (1) [with ξ from equation (3)] by only a factor of $\pi/4$, and equation (7) preserves the time-dependence of fault-slip which is the primary feature of interest here. Booker (1974) used a similar simplification in his study.

It is more convenient to eliminate the infinite range of integration by subtracting from equation (7) its value at $\theta = 0$, that is,

$$\tau_{flt}(\delta_0) = \tau_\infty(0) - \frac{G}{(1 - \nu_u)(2L)} \int_{-\infty}^{0} \frac{d\delta}{d\theta}(\theta') L(\theta - \theta')\, d\theta'$$

where $\delta_0 = \delta(0)$ and πa has been replaced by $2L$. The result is

$$\frac{2L(1 - \nu)}{G} \{\tau_\infty(\theta) - \tau_\infty(0) - [\tau_{flt}(\delta(\theta)) - \tau_{flt}(\delta_0)]\}$$

$$= r(\delta - \delta_0) - (r - 1) \int_0^{\theta} \frac{d}{d\theta}(\delta - \delta_0) K(\theta - \theta')\, d\theta' \tag{9}$$

where $r = (1 - \nu)/(1 - \nu_u)$, and $K(\xi) = \xi[1 - \exp(-1/\xi)]$. The parameter r is the ratio of the stiffness of response of the surrounding material for undrained conditions to that for drained conditions (see Figures 3 and 4). A detailed discussion of appropriate values for ν and ν_u and, thus, of r has been given by RR. Choosing $r = \frac{4}{3}$ corresponding to $\nu = 0.2$ and $\nu_u = 0.4$ and $r = \frac{8}{7}$ corresponding to $\nu = 0.2$ and $\nu_u = 0.3$ brackets the range of interest, but as noted by RR there seems to be no direct source of *in situ* values of ν and ν_u. Rice and Cleary (1976) and O'Connell and Budiansky (1977) have remarked that values inferred from seismic wave speed ratios are not appropriate, and the effects of large scale joints and fractures in the field are likely to cause *in situ* values to differ substantially from those inferred from intact laboratory specimens as in Rice and Cleary (1976).

As remarked earlier, there have been very few precise laboratory determinations of the relation for stress versus relative sliding, and in addition, it is at present not known how accurately such experimentally determined constitutive relations reflect

in situ conditions. In view of these uncertainties, we have simply assumed that the τ_{flt} versus δ relation is parabolic in the vicinity of peak stress (Figure 4)

$$\tau_{flt}(\delta) = \tau_p - (\tau_p - \tau_r)[(\delta - \delta_p)^2/(\delta_r - \delta_p)^2], \quad \delta > \delta_0. \tag{10}$$

The peak stress τ_p occurs at δ_p and at an amount of slip δ_r the parabola is truncated since the stress typically levels off at a residual value τ_r. There is no slip beyond the initial value δ_0 until a threshold stress $\tau_{flt}(\delta_0)$ is reached and in practice $\delta_0 \simeq \delta_p$ as experiments suggest that the stress drops with even very small amounts of relative displacement. This curve has the character of those observed by Dieterich (1978) and by Barton (1972, 1973), but details of the shape are uncertain.

Substituting equation (10) into equation (9) with $\delta_0 = \delta_p$ and rearranging yields

$$Q\theta + r\hat{\delta}^2/2 = r\hat{\delta} - (r - 1)\int_0^\theta \frac{d\hat{\delta}}{d\theta'}(\theta')\, K(\theta - \theta')\, d\theta' \tag{11}$$

where $\hat{\delta} = (\delta - \delta_p)/(\delta_B - \delta_p)$, δ_B is the value of δ at which final instability (dynamic

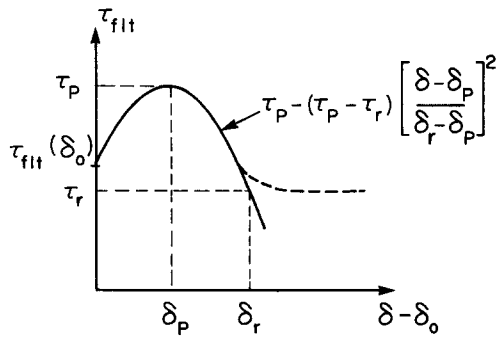

FIG. 4. Assumed form of τ_{flt} versus relative slip relation. The dashed portion of the curve illustrates a more realistic leveling off at a residual level of stress. It was assumed in the calculations that $\delta_0 = \delta_p$.

runaway of fault slip) occurs,

$$Q = 2(1 - \nu)(1 - \nu_u)\left[\frac{(2L)^2}{4\pi^2 c}\right]\left[\frac{\dot{\tau}_\infty}{G}\right]\left[\frac{(\tau_p - \tau_r)(2L)^2}{G(\delta_r - \delta_p)^2}\right] \tag{12}$$

and $\dot{\tau}_\infty$ has been taken as constant. The first bracket in equation (12) contains the characteristic diffusion time (length squared divided by diffusivity) but it is important to note that an additional factor of $(2L)^2$ enters the last bracket. Thus, Q is proportional to the fault length to the fourth power. The second bracket in equation (12) is the far-field strain-rate so that the product of the first two square brackets is the ratio of the characteristic time for diffusion to that for tectonic straining. This ratio is typically very small. The last bracket contains parameters of the constitutive law.

A simple numerical procedure for solving equation (11) is outlined in the Appendix and the results are given in the next section.

Numerical Results for Precursor Time

Equation (11) has been solved for a wide range of values for the loading parameter Q and for two values of the stiffness ratio r. Typical histories of slip versus time nondimensionalized by the diffusion time $t_D = (2L)^2/4c\pi^2$ are shown in Figures 5 and 6 for $Q = 0.35$ and for $r = \frac{4}{3}$ and $r = \frac{8}{7}$, respectively. The dashed curves show the corresponding slip in the absence of pore fluid effects. The nondimensional precursor time θ_{prec} is defined as in RR as the time which elapses between the slip at which instability would occur in the absence of pore fluids (point A) and that (point B) at which instability ultimately occurs. Thus, points A and B correspond to the same points in Figure 3. There is, of course, some arbitrariness in the definition of precursor time, but the definition is unambiguous within the context of the model

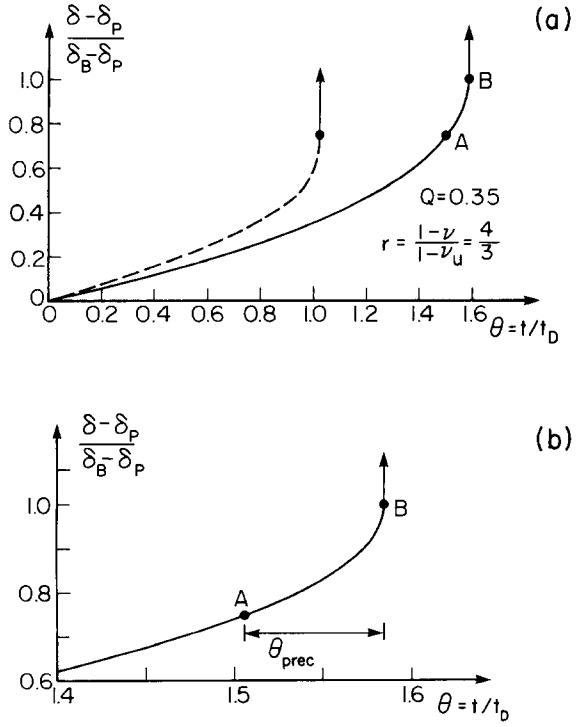

FIG. 5. History of time-dependent fault slip for constant $\dot{\tau}_\infty$. A and B are as in Figure 3a. δ_β is the value of slip at B. Dashed curve is the slip history in the absence of pore-fluid effects.

and, as remarked earlier, this is the period during which the time scale of deformation is set by pore-fluid diffusion rather than the tectonic strain rate so that precursory effects may be detectable. Although instability in the absence of pore fluids is preceded by accelerated slip, Figures 5 and 6 make it clear that the effect is much more pronounced with coupled deformation diffusion effects. The variation of θ_{prec} with Q is shown in Figure 7. Note that θ_{prec} increases with decreasing Q, but θ_{prec} appears to have no simple functional relation to Q. As is to be expected, θ_{prec} is smaller for the smaller value of r.

Some results are shown in dimensional form in Table 1 for $r = \frac{4}{3}$ and in Table 2 for $r = \frac{8}{7}$. Three values of fault length ($2L$) 1 km, 3 km, and 5 km, and two values of the diffusivity, $c = 0.1$ m^2/sec and $c = 1$ m^2/sec are shown. Relatively small values of the fault length have been chosen because the analysis neglects the effects of the

free surface which will be more significant for faults of larger dimension. The diffusivities are representative of those inferred from field observations of faulting phenomena and they have been discussed in more detail by Rice and Simons (1976). Geodetic measurements of the rate of strain accumulation on the San Andreas (Prescott and Savage, 1976) suggest $\dot{\tau}_\infty = 0.1$ bar/yr. A representative value of $\tau_p - \tau_r$ might be 100 bars and $G = 200$ kb. Rice (1977) has inferred a value of $\delta_r - \delta_p \doteq 2$ to 3 μm from Dieterich's (1978) study of slip on flat ground surfaces of Westerly granite and a $\delta_r - \delta_p$ value of 2 − 3 mm from Coulson's results (quoted by Barton, 1973) for shear of a natural joint in granite. However, because these results suggest that $\delta_r - \delta_p$ increases with the presence of gouge and, possibly, with length of sliding surface (Barton, 1972), a value of $\delta_r - \delta_p = 2$ cm has been chosen as representative of *in situ* conditions. In any case, $\delta_r - \delta_p$ is the most uncertain of the parameters

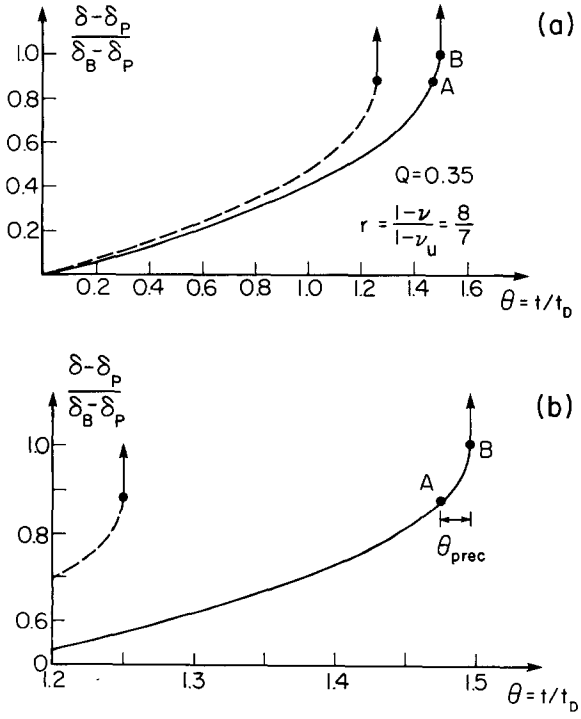

FIG. 6. Same as Figure 5 except the stiffness ratio $r = \frac{8}{7}$.

and, unfortunately, the calculation is sensitive to its value because it appears squared in the denominator of the expression for Q. Of course, the effects of alterations in parameters can be determined from Figure 7, but the precise measurements of stress-displacement curves under a variety of conditions would certainly be a worthwhile undertaking.

DISCUSSION

Examination of Tables 1 and 2 indicates that an increase in the stiffness ratio r from $\frac{8}{7}$ to $\frac{4}{3}$ causes a three- to fivefold increase in t_{prec}. An order of magnitude decrease in diffusivity c from 1 m^2/sec to 0.1 m^2/sec causes an increase in t_{prec} of 1.2 to 3 times. The most interesting feature of the results, however, is that the predicted precursor time in days t_{prec} not only is not proportional to the diffusion time t_D =

$L^2/c\pi^2$ but actually decreases with increasing values of t_D. This result is caused by the dependence of Q on $(2L)^4$ [see equation (12)] whereas $t_D \propto (2L)^2$ and, more fundamentally, by the dependence on L of the stiffness of the surrounding material (as reflected in Figure 2 by the slope of the Eshelby line). Because the constitutive law introduces into the driving force Q an additional characteristic length $\delta_r - \delta_p$ which must be scaled by the fault length, Q increases much more rapidly with L than does t_D. This rapid increase in Q can therefore outweigh the increase in t_D and cause t_{prec} to decrease with increasing L.

It will be shown here that the increase of t_{prec} with fault length agrees with the limiting case of RR's results for stabilization of a narrow inclusion-like fault zone by time-dependent stiffness of the surroundings. Although the analysis of RR applied

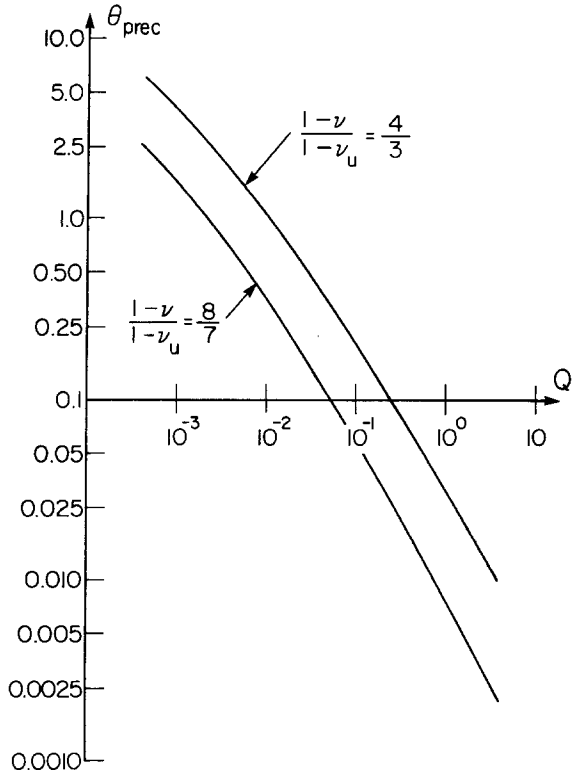

FIG. 7. Prescursor time nondimensionalized by the diffusion time as a function of the nondimensional loading parameter Q [see equation (12)].

rigorously for spherical inclusions, the results for narrow axisymmetric inclusions were approximated simply by choosing an appropriate slope for the Eshelby line. A comparison of their results with those here requires the conversion of the relative slip δ to a measure of shear strain for a narrow elliptical (plane strain) inclusion. If the semiaxes of the ellipse are L and b, where $L \gg b$, then $\delta/2b$ yields a measure of strain in the narrow inclusion. The width of the peak in the stress-strain curve, which was assumed by RR to be parabolic near peak stress [see equation (3) or Figure 6 of RR], was λ. This λ can be related to the parameters of the τ versus δ curve (Figure 4) by requiring that the difference in strain, as measured here by $\delta/2b$, between the values at peak stress and at final instability (undrained runaway) be the same in both cases. Then a comparison of equation (10) with equation (31) of

RR reveals that

$$\lambda = \frac{G}{(\tau_p - \tau_r)} \left[\frac{\delta_r - \delta_p}{2L} \right]^2 \eta^2 \tag{13}$$

where $\eta = L/b$ is the aspect ratio of the inclusion. For $\eta = 18$ as assumed by RR and the values used in Tables 1 and 2

$$\lambda = \frac{1.3 \times 10^{-4}}{(2L \text{ in km})^2}. \tag{14}$$

For the fault zone sizes used here and by RR, the values of λ from equation (14) are

TABLE 1

PREDICTED PRECURSOR TIME t_{prec} IN DAYS FOR THE TRANSITION FROM A TO B IN FIGURE 3a*

	$2L$ = 1 km	$2L$ = 3 km	$2L$ = 5 km
$c = 1$ m^2/sec	$Q = 4.8 \times 10^{-4}$	$Q = 3.9 \times 10^{-3}$	$Q = 0.3$
	$t_D = 0.29\ d$	$t_D = 2.64\ d$	$t_D = 7.33\ d$
	$\theta_{prec} = 5.75$	$\theta_{prec} = 0.40$	$\theta_{prec} = 0.087$
	$t_{prec} = 1.69\ d$	$t_{prec} = 1.05\ d$	$t_{prec} = 0.64\ d$
$c = 0.1$ m^2/sec	$Q = 4.8 \times 10^{-3}$	$Q = 3.9 \times 10^{-1}$	$Q = 3.0$
	$t_D = 2.93\ d$	$t_D = 26.4\ d$	$t_D = 73.3\ d$
	$\theta_{prec} = 1.62$	$\theta_{prec} = 0.072$	$\theta_{prec} = 0.0128$
	$t_{prec} = 4.75\ d$	$t_{prec} = 1.91\ d$	$t_{prec} = 0.94\ d$

* The following values were used in the calculation: $\dot{\tau}_\infty = 0.1$ bar/yr, $G = 200$ kb, $\tau_p - \tau_r = 100$ bars, $\delta_r - \delta_p = 2$ cm, $r = 4/3$. Also shown are Q, the nondimensional forcing term [equation (12)]; the diffusion time $t_D = L^2/c\pi^2$ in days, and the nondimensional precursor time $\theta_{prec} = t_{prec}/t_D$.

TABLE 2

SAME AS TABLE 1 EXCEPT THE STIFFNESS RATIO $r = 8/7$

	$2L$ = 1 km	$2L$ = 3 km	$2L$ = 5 km
$c = 1$ m^2/sec	$Q = 5.6 \times 10^{-4}$	$Q = 4.55 \times 10^{-2}$	$Q = 0.35$
	$t_D = 0.29\ d$	$t_D = 2.64\ d$	$t_D = 7.33\ d$
	$\theta_{prec} = 2.24$	$\theta_{prec} = 0.115$	$\theta_{prec} = 0.021$
	$t_{prec} = 0.66\ d$	$t_{prec} = 0.30\ d$	$t_{prec} = 0.15\ d$
$c = 0.1$ m^2/sec	$Q = 5.6 \times 10^{-3}$	$Q = 4.55 \times 10^{-1}$	$Q = 3.5$
	$t_D = 2.93\ d$	$t_D = 26.4\ d$	$t_D = 73.3\ d$
	$\theta_{prec} = 0.575$	$\theta_{prec} = 0.017$	$\theta_{prec} = 0.0024$
	$t_{prec} = 1.69\ d$	$t_{prec} = 0.44\ d$	$t_{prec} = 0.18\ d$

20 to 500 times smaller than the value (25×10^{-4}) used by RR. This discrepancy again emphasizes the need for precise investigations of constitutive parameters both for the deformation of intact rock and for frictional sliding.

If equation (14) is used in equation (35) in RR which is their expression for the nondimensional driving force denoted by R [analogous to Q in equation (11)], then

$$R \propto (2L)^4.$$

Because R then has the same dependence on L as does Q, the predicted decrease in t_{prec} with increasing t_D agrees with the proper limit of the result for a narrow inclusion having a fixed parabolic τ versus δ relation. (This result was suggested to me in a personal communication from J. R. Rice.) When equation (14) is substituted into equation (35) of RR, values of t_{prec} predicted here can be compared with those estimated from Figure 12 of RR. (Note that estimates are necessary because RR

gives curves corresponding to $r = 1.1$ and 1.25.) For $c = 1$ m^2/sec, $r = \frac{8}{7}$, $\dot{\tau}_\infty = 0.1$ bar/yr and values for the fault length of 1 km and 5 km, t_{prec} estimated from the curve for $r = 1.1$ in Figure 12 of RR are 0.41 d and 0.18 d, respectively. The corresponding values from Table 2 are 0.66 and 0.15 d. The agreement is very good. Although it is not surprising that an axisymmetric inclusion of aspect ratio 18:1 adequately models a very narrow fault zone, the good agreement does suggest that the primary effect of geometry is on the stiffness of the surrounding material and that differences in the details of the induced flow field (for plane strain versus axisymmetric deformation) do not greatly alter the relaxation time from undrained to drained response.

The prediction that the precursor time decreases with increasing size of the fault zone appears to disagree with studies based on field observations (e.g., Figure 5 of Whitcomb *et al.*, 1973; Figure 3 of Anderson and Whitcomb, 1975; Figure 9 of Scholz *et al.*, 1973). Nevertheless, the scatter in those data for small fault lengths, for which the results calculated here are most applicable, would not seem to rule out a precursor time which is constant or decreases slightly with fault length. As remarked earlier, events on larger faults are likely to be complicated by effects of the free surface and by the possibly time-dependent boundary condition on the base of the lithosphere. Moreover, this analysis has neglected the complementary stabilizing mechanism of dilatant hardening and has assumed that the significant inelasticity is confined to a very narrow zone. The latter evidently cannot be the case if observations of wave-speed travel-time anomalies are to be attributed to dilatancy: a substantial proportion of the material sampled by the wave path must be dilatant. Dilatancy may arise from uplift in sliding on the fault surface and laboratory observations (e.g., Barton, 1973) suggest that such uplift can be suppressed only by a compressive stress on the order of the strength of intact rock. An additional source of dilatancy is the inelastic deformation near the ends of the faults due to the strong stress concentrations there. The accompanying stabilizing effects due to dilatant hardening may cause the precursor time to scale with fault length in a way which is different from predictions based on only the stabilization due to the time-dependent stiffness effect.

The predictions for the precursor time in Tables 1 and 2 are very short and observed effects due to accelerated slip prior to instability would provide short-time precursors. In addition, the magnitude of the effects will diminish approximately as the inverse square of the distance from their source. Thus, the increase in deformation rate over the background tectonic rate may be detectable at the free surface only toward the end of what is called here the precursory period. If $\delta_r - \delta_p$, the slip necessary for the fault stress to decrease from peak to residual value (Figure 4), is much smaller than the 2-cm value assumed here, the predicted precursor times will be very much shorter. Indeed, even if the complementary stabilizing effect due to dilatant hardening is included, there is the possibility that precursor times may be too short to be detectable in practice, for example, by strain or tiltmeters. This is one possible explanation for the frequent failure to observe precursory effects.

The results here and those of RR strongly suggest that the coupling of pore-fluid diffusion with deformation will be important in setting a time scale for processes preparatory to faulting. At the same time, precise predictions are impossible in view of uncertainties about constitutive parameters and transport properties.

Acknowledgments

I thank J. R. Rice for suggesting this research and for many helpful discussions. C. Showers was instrumental in performing the numerical calculations leading to Figures 5, 6, and 7 and W. D. Stuart

made several helpful comments on the manuscript. This research was supported by the U.S.G.S Earthquake Hazards Reduction Program through Grant 14-080001-16795. Support from the Department of Theoretical and Applied Mechanics at the University of Illinois at Urbana is also gratefully acknowledged.

REFERENCES

Anderson, D. L. and J. H. Whitcomb (1975). Time-dependent seismology, *J. Geophys. Res.* **80,** 1497–1503.

Barton, N. (1972). A model study of rock-joint deformation, *Int. J. Rock Mech. Mining Sci.* **9,** 579–602.

Barton, N. (1973). Review of a new strength criterion for rock joints, *Eng. Geol.* **7,** 287–332.

Bilby, B. A. and J. D. Eshelby (1968). Dislocations and the theory of fracture, in *Fracture*, vol. 1, H. Liebowitz, Editor, Academic Press, New York, 99–182.

Booker, J. R. (1974). Time-dependent strain following faulting of a porous medium, *J. Geophys. Res.* **79,** 2037–2044.

Cleary, M. P. (1976). Continuously distributed dislocation model for shear bands in geological materials, *Numerical Methods Eng.* **10,** 679–702.

Cleary, M. P. (1977). Fundamental solutions for a fluid saturated porous solid, *Intern. J. Solids Struct.* **13,** 785–806.

Dieterich, J. H. (1978). Time-dependent friction and mechanics of stick-slip, *Pure Appl. Geophys.* **116,** 790–806.

Muskhelishvili, N. I. (1953). *Singular Integral Equations*, J. R. M. Radok, Translator, Noordhoff, Groningen, Holland.

Nur, A. (1972). Dilatancy, pore fluids, and premonitory variations of travel times, *Bull. Seism. Soc. Am.* **78,** 1217–1222.

O'Connell, R. J. and B. Budiansky (1977). Viscoelastic properties of fluid-saturated cracked solids. *J. Geophys. Res.* **82,** 5719–5735.

Prescott, W. H. and J. C. Savage (1976). Strain accumulation on the San Andreas fault near Palmdale, California, *J. Geophys. Res.* **81,** 4901–4908.

Rice, J. R. (1973). The initiation and growth of shear bands, in *Plasticity and Soil Mechanics*, A. C. Palmer, Editor, Cambridge University Engineering, Cambridge, England, 263–274.

Rice, J. R. (1977). Theory of precursory processes in the inception of earthquake rupture, *Beitr. Geophysik* (in press).

Rice, J. R. and M. P. Cleary (1976). Some basic stress diffusion solutions for fluid-saturated porous media with compressible constitutents, *Rev. Geophys. Space Phys.* **14,** 227–241.

Rice, J. R. and D. A. Simons (1976). The stabilization of spreading shear faults by coupled deformation-diffusion effects in fluid-infiltrated porous materials, *J. Geophys. Res.* **81,** 5322–5334.

Rice, J. R. and J. W. Rudnicki (1979). Earthquake precursory effects due to pore fluid stablization of a weakening fault zone, *J. Geophys. Res.* (in press).

Rice, J. R., J. W. Rudnicki, and D. A. Simons (1978). Deformation of spherical cavities and inclusions in fluid-infiltrated elastic solids, *Intern. J. Solids Struct.* **14,** 289–303.

Rudnicki, J. W. (1977). The inception of faulting in a rock mass with a weakened zone, *J. Geophys. Res.* **82,** 844–854.

Scholz, C. H., L. R. Sykes, and Y. P. Aggarwal (1973). Earthquake prediction: a physical basis, *Science* **181,** 803–810.

Stuart, W. D. (1979a). Strain softening prior to two dimensional strike-slip earthquakes, *J. Geophys. Res.* **84,** 1063–1070.

Stuart, W. D. (1979b). Strain softening instability model for the San Fernando earthquake, *Science* **203,** 907–910.

Stuart, W. D. and G. M. Mavko (1979). Earthquake instability on a strike-slip fault, *J. Geophys. Res.* (in press).

Whitcomb, J. H., J. D. Garmany, and D. L. Anderson (1973). Earthquake prediction: variation of seismic velocities before the San Fernando earthquake, *Science* **180,** 632–635.

SEISMOLOGICAL LABORATORY
DIVISION OF GEOLOGICAL AND PLANETARY SCIENCES
CALIFORNIA INSTITUTE OF TECHNOLOGY
PASADENA, CALIFORNIA 91125
CONTRIBUTION NO. 3188

Manuscript received November 6, 1978

APPENDIX

Numerical solution of equation (11)

The integral in equation (11) can be discretized by writing

$$I = \int_0^{\theta} \frac{d\hat{\delta}}{d\theta'}(\theta)\, K(\theta - \theta')d\theta' = \sum_{k=1}^{n} \int_{(k-1)\Delta\theta}^{k\Delta\theta} \frac{d\hat{\delta}}{d\theta'}(\theta')K(\theta - \theta')d\theta'$$

where $\theta = n\Delta\theta$. If the derivative $d\hat{\delta}/d\theta'$ is approximated as constant in each interval,

$$I \simeq \delta_n K_1 + \sum_{l=1}^{n-1} \delta_{n-l}(K_{l+1} - K_l) \tag{A1}$$

where $\delta_k = \hat{\delta}(k\Delta\theta)$ and

$$K_l = \Delta\theta \int_{(l-1)}^{l} u[1 - \exp(-1/u\Delta\theta)]du.$$

The K_l can be computed numerically and the substitution of equation (A1) into equation (11) yields a quadratic equation for δ_n.